Chapter 2

Dissimilar Metal Joining of Zinc Coated Steel and Aluminum Alloy by Laser Roll Welding

Hitoshi Ozaki and Muneharu Kutsuna

Additional information is available at the end of the chapter

http://dx.doi.org/10.5772/48242

1. Introduction

Nowadays, the car industry has targets to improve fuel consumption due to the problems of the global environment. For example, in the Corporate Average Fuel Economy, CAFE, which was approved in the U. S. Congress in July 2011, attaining the average fuel efficiency of 54.5 mpg (23.2 km/l) by 2025 is called for (Yamamoto, 2012). In addition, it's obliged to improve the average fuel efficiency to 35.5 mpg (15.1 km/l) by 2017. This is a significant increase compared with the present 27.5 mpg (11.7 km/l) which have been fixed for the past 11 years. Hence, the further weight reduction of cars has become imperative.

On the other hand, the weight of vehicle which influences the fuel consumption directly is increasing owing to a rise of safety awareness of automobile user's, tightening of safety standards, and diversification and sophistication of needs. Therefore, the car industry has conflicting targets of the low fuel consumption by "lightening car body" and "safety improvement". Additionally these targets should be achieved in together. Then, a "hybrid body structure" concept has been proposed.

In this concept, high strength steel and light alloy are arranged in the right places of the car body. For instance, by using high strength steel for pillars, a lightening with improving strength is achieved. In addition, by using aluminum alloys for the bonnet, the door panel, and the trunk lid, a further lightening is achieved. In order to make this "hybrid body structure", the welding technology for joining of steel to aluminum with high reliability and productivity is required. However, it's difficult to join steel to aluminum by conventional fusion welding.

Generally, in respect to dissimilar metal joining by the fusion welding, because of melting and alloying largely both metals, intermetallic compound layer formed at joint interface grows thick; oxide firm is formed; hot cracking is generated. Consequently, high joint

strength can not be gotten. Moreover, when melting point of both metals has large difference, burn-through occurs in the metal of lower melting point (Nishimoto et al., 2005).

In order to solve these problems, many studies of the dissimilar metal joining have been conducted such as resistance welding (Okita, 2004), laser welding (Katayama, 2004), explosive welding (Satou, 2004), friction stir welding (Okamura & Aota, 2004; Katoh & Tokisue, 2004), and diffusion bonding (Ohashi, 2004). As a result, solid-phase bonding is mainly put to practical use. However, higher productivity, joint strength and flexibility are needed to expand the coverage of application of the dissimilar metal joints. Since laser welding has advantages such as local heat input, short process time and high flexibility compared with other welding processes, there has been considerable research on the welding of steel and aluminum. In the recent, the studies of keyhole welding (Torkamany, et al., 2010), laser welding-brazing (Dharmendra, et al., 2011), dual-beam YAG laser welding (Yan, et al., 2010), and thermal cycle during laser welding (Fan, et al., 2011) are carried out.

Then, the welding process of steel and aluminum which have been regarded as difficult, Laser Roll Welding has been developed for joining of dissimilar metals by M. Kutsuna, M. Rathod and A. Tsuboi in 2002. This welding is a hybrid welding process, as shown in Fig.1, combined high-temperature heating by a 2.4 kW CO_2 laser with pressurizing by a pressure roller. It's registered as Japanese Patents No. 3535152 and No. 3692135.

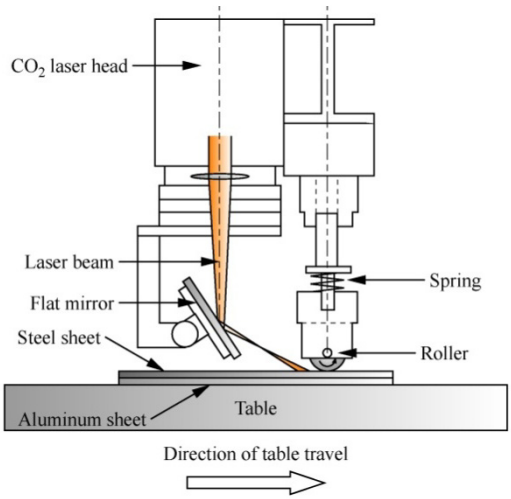

Figure 1. Schematic diagram of Laser Roll Welding process

Fig.2 shows Fe-Al phase diagram (Massalski, et al., 1986). In this figure, there are varioius intermetallic compounds, hereafter, called as IMC's, and they are grouped as Fe-rich compounds, FeAl and Fe_3Al, and Al-rich compounds, $FeAl_2$, Fe_2Al_5 and $FeAl_3$. M. Yasuyama et al. (1996) have shown the mechanical properties of these IMC's. Vickers hardness of cast IMC's is shown in Table 1, and mechanical properties by compressive test are shown in Fig.3.

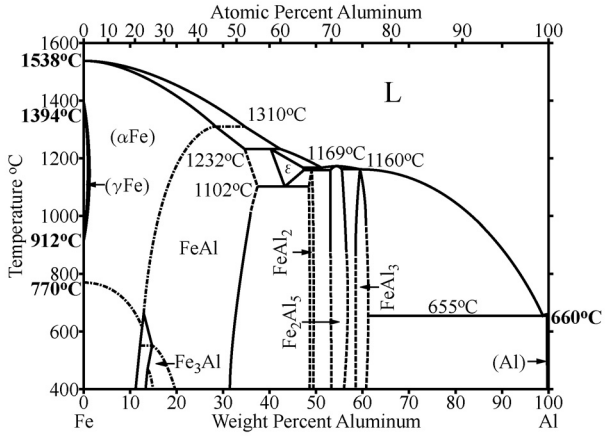

Figure 2. Fe-Al binary equilibrium diagram

	Vickers hardness
$FeAl_3$	892
Fe_2Al_5	1013
FeAl	470
Fe_3Al	330

Table 1. Vickers hardness of Fe-Al intermetallic compounds

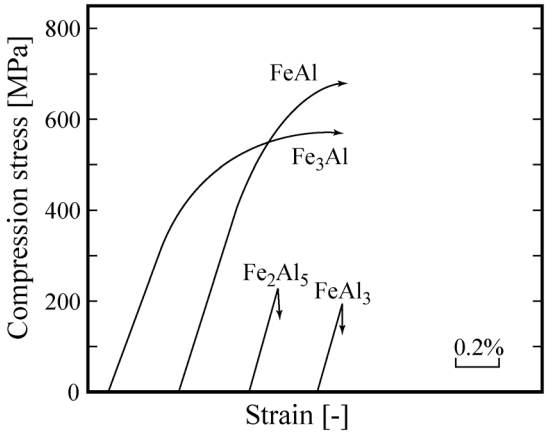

Figure 3. Stress-strain curves in compressive test of Fe-Al intermetallic compounds

While Al-rich IMC's are hard and brittle, Fe-rich IMC's show slight ductility and high strength. These brittle IMC's constitute barriers to the dissimilar metal welding of steel to

aluminum. Kutsuna et al. thought if the thickness of brittle IMC layer is minimized and the formation of more ductile IMC's is promoted, high reliable joints are able to be obtained. Therefore, they developed the Laser Roll Welding process. In this process, since the thermal cycle for joining can be shortened by laser heating, the formation of the brittle IMC's can be easily controlled. Furthermore, good contact of a steel sheet and an aluminum sheet and rapid heat transfer from the steel sheet to the aluminum sheet are conducted by the pressure roller.

Kutsuna et al. produced Laser Roll Welidng equipment experimentally, and conducted basic studies of the welding of low carbon steel to aluminum alloy (Rathod &Kutsuna, 2003, 2004). As a result, when the IMC layer thickness was from 4 to 8 μm, failure of base metal sheet was obtained after tensile shear test of specimen.

Until now, it's found that Laser Roll Welding has two types of welding mechanisms. The combination of iron and aluminum is that of metals with large difference in their melting points (Ozaki & Kutsuna, 2007). The combination of titanium and aluminum also corresponds to this category (Ozaki et al., 2008). In this case, only the metal with a higher melting point is heated up to an elevated temperature for avoid the formation of brittle IMC's. For example, in the case of steel to aluminum joint, steel is heated up to 1200 ^{o}C, because the max formation temperature of Fe_2Al_5 is 1169 ^{o}C. The interlayer is formed and cooled rapidly to minimize the thickness of brittle IMC's.

The other is a combination of metals with eutectic reaction at a lower temperature than melting point. For instance, the combination of titanium and iron falls into this type (Ozaki et al., 2007). In this case, the eutectic reaction occurs at a lower temperature, about 1085 ^{o}C, than melting points of both metals. The interlayer of the eutectic phase, β-Ti and TiFe, is formed at the interface.

In this way, uncoated materials have been mainly used in the previous study of Laser Roll Welding. However, coated materials such as zinc coated steel have not investigated enough yet. In this chapter, Laser Roll Welding of zinc coated steel and 6000 series aluminum alloy was conducted, and the weldability was investigated. Two types of zinc coated steel were used. One is hot-dip galvanized steel called as GI, the other is hot-dip galvannealed steel called as GA. The former is used mainly in Europe, the latter is in Japan. Then, the influences of process parameters, such as welding speed and roll pressure, on the formation of intermetallic compound layer and the change of zinc coated layer have been investigated to get sound joints with these galvanized steel. Furthermore, the effects of process parameters on joint performance have been also discussed.

2. Experimental procedure

2.1. Materials used

As materials, two types of zinc coated steel and A6000 series aluminum alloy, Al-0.5Mg-1.0Si, were used for joining. The zinc coated steels were hot-dip galvanized steel, hereafter,

called as GI, and hot-dip galvannealed steel, hereafter, called as GA, respectively. The dimension of the zinc coated steel sheets were 125 x 180 x 0.55 mm and that of the A6000 series aluminum alloy sheet, hereafter, called as A6000, was 125 x 180 x 1 mm. The zinc coating weight of the GI sheet was 60 g/m^2 and the GA was 45 g/m^2.

The surface of the steel sheets was coated with graphite by using a graphite spray to increase the absorption rate of laser beam. The thickness of the coating layer was approximately 10 μm. The faying surface of the steel sheets was only degreased with ethanol alcohol. The faying surface of the A6000 sheet was wire-brushed, polished by emery paper #600 and cleaned by ethanol before welding. Then, to remove the oxide firm on aluminum alloy sheet, the surface of the aluminum alloy was spread with flux, $KAlF_4$:$K_2AlF_5 \cdot H_2O$, 17-25 wt%, with particle size of 15 to 21 μm.

The setup of specimens is shown in Fig.4. A zinc coated steel sheet is placed as a top plate; an A6000 sheet is placed as a bottom with 3 mm width overlapping.

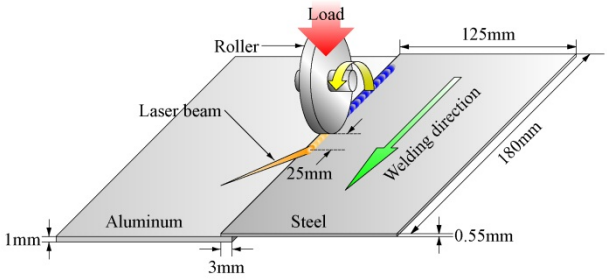

Figure 4. Setup of specimens in Laser Roll Welding

Laser type	CO_2 laser (Pulse mode)
Laser peak power	2.0 kW
Duty cycles	75%
Frequency	150 Hz
Beam spot size	Minor axis : 2.5 mm Major axis : 3.5 mm
D_{LR}	25 mm
Welding speed	3.3 ~ 15.0 mm/s
Overlapped width	3 mm
Roll pressure	100 ~ 175 MPa
Shielding gas	Ar : 25 l/min

D_{LR}: Distance between Laser beam spot and Roller

Table 2. Process parameters for Laser Roll Welding

2.2. Process parameters

In this study, to investigate the effect of the welding condition on the joint properties of two types of zinc coated steel and aluminum alloy by Laser Roll Welding, welding speed and roll pressure were varied. Process parameters are shown in Table 2.

Pulsed laser was used by controlling a 2.4 kW CO_2 laser with continues wave. Laser peak power, duty cycles and frequency were constant 2.0 kW, 75 % and 150 Hz respectively. These parameters have been optimized in the previous study. Beam spot shape was an quasi-elliptical with major axis of 3.5 mm and minor axis of 2.5 mm. Distance between the center of laser beam spot and the pressurizing axis of roller was 25 mm. Welding speed was varied from 3.3 to 15.0 mm/s. Overlapped width was 3 mm, and laser beam was irradiated the center of overlap. The roller is mounted with a calibrated compression spring for applying predetermined roll pressure. The roll pressure was calculated by assuming that the contact area between the roller and the steel sheet surface was a rectangle of 15 mm^2. Roll pressure was varied from 100 to 175 MPa. For the sake of the protection of condenser lens and the oxidation prevention of Laser Roll Welded joints, argon gas with flow rate of 25 l/min was used.

2.3. Evaluation method of Laser Roll Welded joints

After welding, Laser Roll Welded specimens were cut across the lap joint seam for macrostructure and microstructure observation. Etching with 3% nital was made for observation of the interface layer. Hardness test and electron-probe microanalysis (EPMA) were conducted to analyze the interface layer and to identify the IMC present.

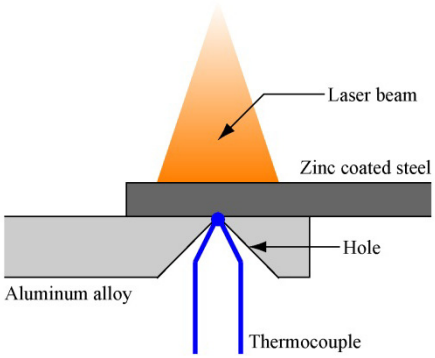

Figure 5. Schematic diagram of measurement method for thermal cycle at weld interface

Thermal cycle was measured using a Pt-PtRh thermocouple with a diameter of 0.3 mm. As shown in Fig.5, a cone-shaped hole of 2 mm in diameter was drilled at the center of the overlap width in the aluminum sheet. The hole was used for placing thermocouple at the lower surface of the steel sheet. In addition, tensile shear test and Erichsen cupping test were carried out to investigate the mechanical properties of welded joint. The specimens with 20 mm width were used for tensile shear test and with 77 mm square for Erichsen cupping test.

3. Experimental results and discussions

3.1. Bead appearance and cross-section of Laser Roll Welded joints

Bead appearance of Laser Roll Welded specimen with the welding speed of 8.3 mm/s and roll pressure of 150 MPa are shown in Figs.6-7. Top bead is shown in Fig.6, and bottom bead is in Fig.7. Furthermore, cross-section of the weld bead is shown in Fig.8. In these figures, (a) shows GI/A6000 joint and (b) shows GA/A6000, respectively.

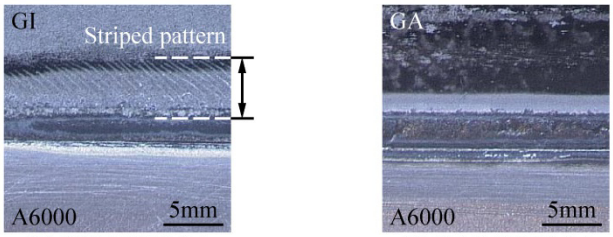

(a) GI/A6000 joint (b) GA/A6000 joint

Figure 6. Top bead appearance of GI/A6000 and GA/A6000 Laser Roll Welded joints

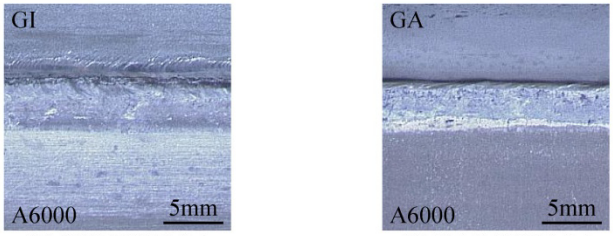

(a) GI/A6000 joint (b) GA/A6000 joint

Figure 7. Bottom bead appearance of GI/A6000 and GA/A6000 Laser Roll Welded joints

(a) GI/A6000 joint (b) GA/A6000 joint

Figure 8. Macro cross-section of GI/A6000 and GA/A6000 Laser Roll Welded joints

As shown in Fig.6, both of the bead turned black due to the effect of the graphite spray and the laser heating. In Fig.6 (a), striped pattern is observed on the GI sheet near the weld bead. This is the first time this striped pattern has been observed in the past study of Laser Roll Welding, the pattern seems to be unique to this welding of galvanized steel sheet. A GI sheet has galvanized layer, which exists as a thin layer at the surface of steel sheet. Thus it's thought that the pattern was caused by the laser heating and the roller pressure. On the other hand, the striped pattern doesn't exist on the GA sheet as

shown in Fig.6 (b). This is because the coated layer of a GA sheet is alloyed zinc with iron.

As shown in Figs.7-8 (a), partial melting and spreading of molten aluminum alloy on the GI sheet occurs in the A6000 sheet. The GI sheet was heated by laser, and the heat transferred to A6000 sheet by the contact of GI and A6000 sheets. Hence A6000 sheet was supposed to be melted. In contrast, molten A6000 alloy doesn't spread on the GA sheet.

In order to compare the wettability of the GI sheet with that of the GA sheet, bonding width was measured from the cross-section of the weld bead as shown in Fig.9 (a). Effect of the welding speed and the roll pressure on the bonding width of GI/A6000 and GA/A6000 joints are shown in Fig.9 (b) and (c), respectively.

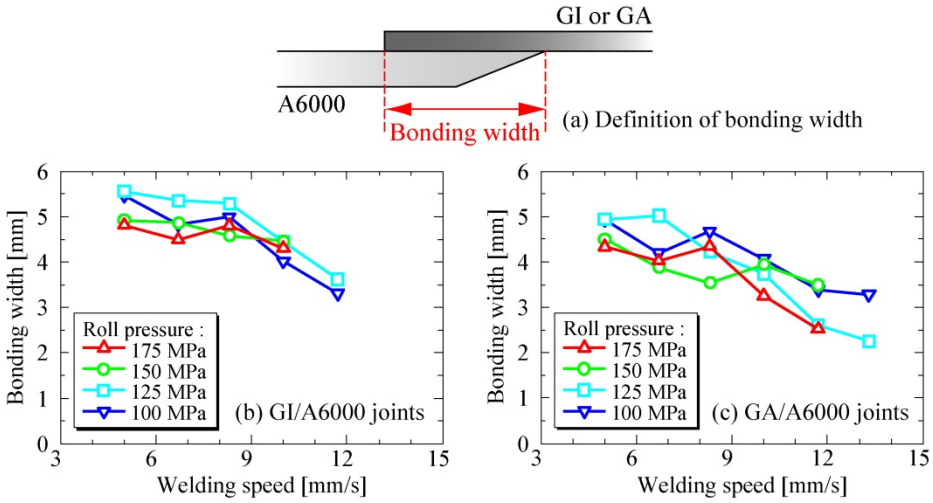

Figure 9. Effect of welding speed on bonding width at different roll pressures

It's common with Fig.9 (b) and (c) that the bonding width decreased as the welding speed is increased from 5.0 to 11.7 mm/s. This is because heat input decreases as the welding speed increased; the meltage of A6000 sheet also decreased. On the whole, the bonding width of GA/A6000 joints is narrower than that of GI/A6000. For example, the width with the welding speed of 8.3 mm/s and roll pressure of 150 MPa of GI/A6000 joint is 4.6 mm, and that of GA/A6000 is 3.5 mm. This is considered to be produced from the difference in the wettability of the surface of the GI and GA sheet.

3.2. Microstructures at weld interface

Interface microstructures of GI/A6000 joint with welding speed of 6.7 mm/s and roll pressure of 150 MPa are shown in Fig.10.

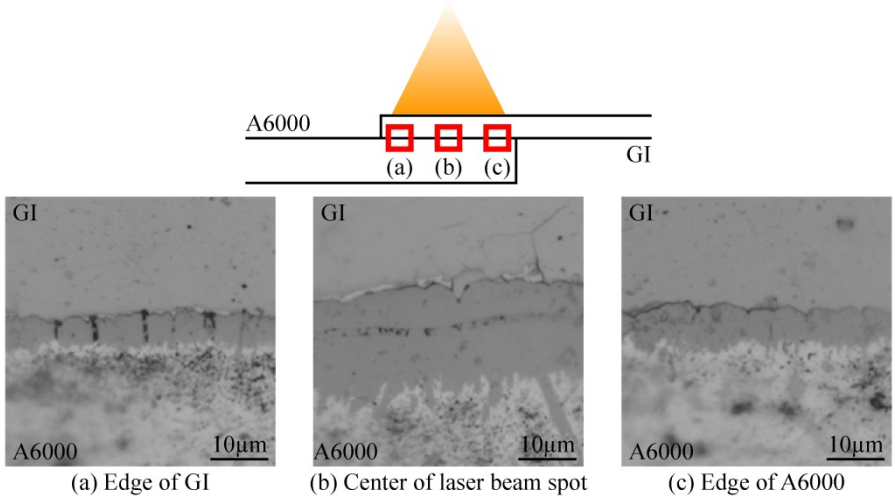

Figure 10. Microstructures at joint interface of GI and A6000 sheet

IMC layer was confirmed at the joint interface between the GI and the A6000 sheet. The IMC layer at the edge of the GI sheet is shown in Fig.10 (a), at the center of the laser beam spot is shown in (b) and at the edge of the A6000 sheet is show in (c). The IMC layer thicknesses in each place were 4.1 μm, 13.0 μm, and 4.9 μm respectively. Therefore, the thickness right under the center of laser beam spot was the thickest. Due to the high energy density near the center of the beam spot of the CO_2 laser used, it's thought that the area under the center of the beam spot is heated the highest temperature and cooled the slowest speed.

Interface microstructures of GA/A6000 joint with welding speed of 8.3 mm/s and roll pressure of 150 MPa are shown in Fig.11. IMC layer was also observed at the interface between the GA and the A6000 sheet. In addition, the thickness right under the center of laser beam spot was the thickest, and this was the same as that of the case of GI/A6000 joint.

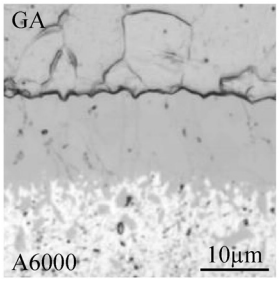

Figure 11. Microstructure at joint interface of GA and A6000 sheet

3.3. Electron-probe microanalysis (EPMA) of interlayer

As the optical microscope doesn't reveal the details of the IMC layers, EPMA of iron, aluminum and zinc across joint interface were made to identify IMC's and existence of zinc. The results for GI/A6000 and GA/A6000 joints at different welding speeds with roll pressure of 150 MPa are shown in Figs.12-13. Bottom pictures show the SEM images of the IMC layer. In these figures, the EPMA results with the welding speed of 8.3 mm/s are shown in (a), with the welding speed of 10.0 mm/s are shown in (b).

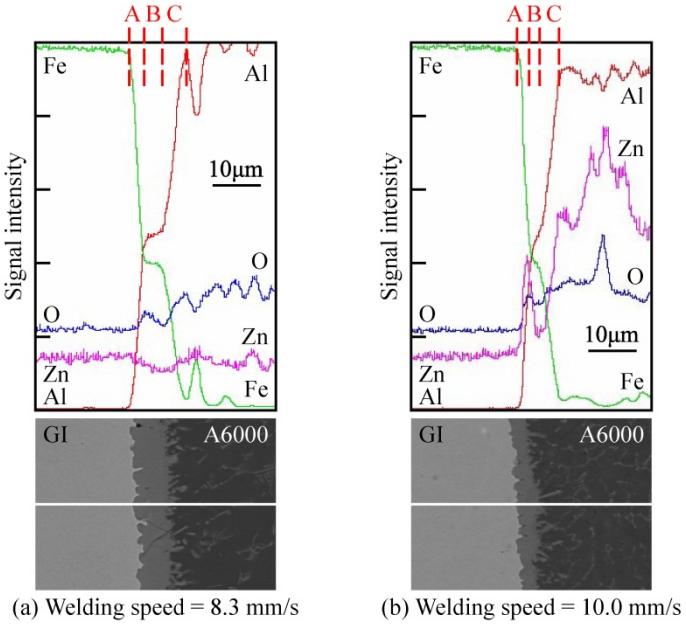

(a) Welding speed = 8.3 mm/s (b) Welding speed = 10.0 mm/s

Figure 12. Results of EPMA at interlayer of GI/A6000 joints

From EPMA results of iron, aluminum and zinc across interface, IMC's and existence of zinc were identified. At the center of these EPMA results which are shown by the layer A to C in Fig.12 as an example, the signal intensity of Fe and Al has changed similarly. At the layer A, the intensity of Fe decreases rapidly, and Al rises. At the layer B, the IMC's are observed as stepped lines. At the layer C, the intensity of Fe decreases further and Al rises. From the estimation of composition from stepped lines at the layer B, it's suggested that main IMC's were brittle $FeAl_3$ and Fe_2Al_5.

When the welding speed is increased to 10.0 mm/s, zinc can be seen in aluminum alloy. From this result, it's thought that zinc tends to diffuse into aluminum when the welding speed becomes more than 10.0 mm/s. This reason is considered as follows.

Most of the zinc layer is vapored by the laser heating from the faying surface of the GI sheet at slow welding speeds. On the other hand, at fast welding speeds, the diffusion amount of

the zinc into aluminum alloy by the roll pressure is larger than the evaporation amount of the zinc by the laser heating.

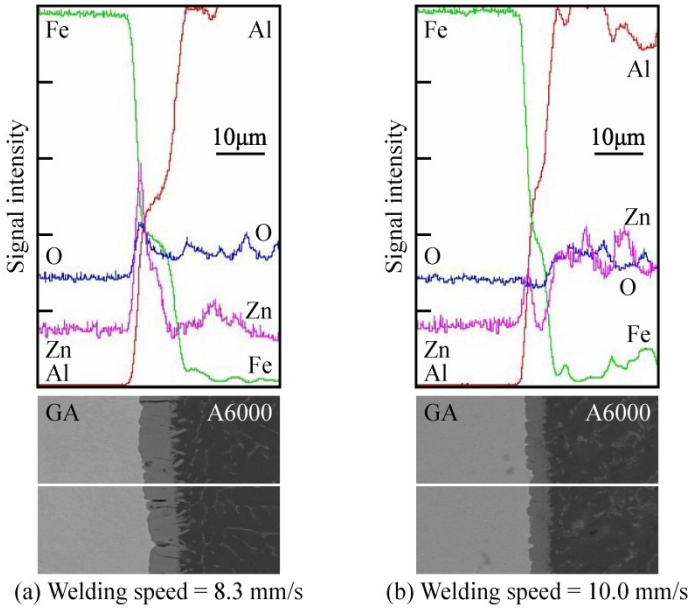

Figure 13. Results of EPMA at interlayer of GA/A6000 joints

As shown in Fig.13 (a), the zinc line has higher peak than any other zinc line at the interface of the GA sheet side. This is because the zinc on GA sheet surface exists as Fe-Zn alloy. Then it's suggested that zinc was hard to be evaporated by the laser heating, and a lot of zinc was remained at the interface of the GA sheet side.

3.4. Vickers hardness measurements

From the EPMA results, it was presumed that main IMC's were brittle $FeAl_3$ and Fe_2Al_5. However, in order to obtain further evidence, Vickers hardness measurement was conducted. SEM image of GI/A6000 and GA/A6000 weld interface after the measurement with welding speed of 8.3 mm/s and roll pressure of 150 MPa are shown in Fig.14 (a) and (b), respectively.

Indentation size became small in order of the base metal of A6000, zinc coated steel, and the IMC layer. In particular, the indentation size of the IMC layer is much smaller than that of both base metals. As shown in Fig.14 (a), the Vickers hardness of the base metal of the GI, the A6000, and the IMC layer were 137 Hv, 94 Hv and 940 Hv on average respectively. The results show a large difference between IMC layer hardness and the surrounding base metals. The IMC hardness was about 10 times more than the A6000 base metal and 7 times more than the GI base metal. In the same way, as shown in Fig.14 (b), the Vickers hardness

of the base metal of the GA, the A6000, and the IMC layer were 141 Hv, 97 Hv and 857 Hv on average respectively, the IMC layer was the hardest. Because the hardness of these IMC layers are between 892 Hv of $FeAl_3$ and 1013 Hv of Fe_2Al_5 according to Table 1, it's thought that $FeAl_3$ and Fe_2Al_5 are mainly formed at the interface as above.

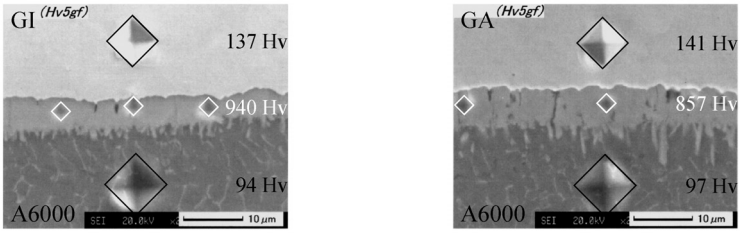

(a) GI/A6000 joint (b) GA/A6000 joint

Figure 14. Results of Vickers hardness measurement at joint interface

3.5. Effect of welding speed on thickness of intermetallic compound layer

Effect of the welding speed on the IMC layer thickness of GI/A6000 and GA/A6000 joints at different roll pressure are shown in Fig.15 (a) and (b), respectively. The thicknesses were measured right under the center of the laser beam spot.

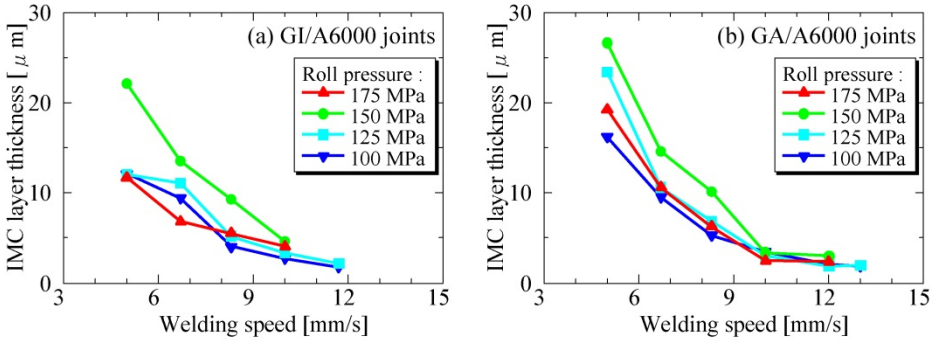

Figure 15. Effect of welding speed on IMC layer thickness of Laser Roll Welded joints interface

The IMC layer thickness decreases significantly as the welding speed is increased from 5.0 to 11.7 mm/s regardless of the roll pressure as shown in Fig.15 (a) and (b). This is because heat input decreases as the welding speed in increased. Therefore, this result indicates that the IMC layer thickness could be suppressed by heat input as was mentioned in previous study of Laser Roll Welding of steel to aluminum alloy.

3.6. Effect of roll pressure on thickness of intermetallic compound layer

Effect of the roll pressure on the IMC layer thickness of GI/A6000 and GA/A6000 joints at constant welding speed of 8.3 mm/s is shown in Fig.16.

The IMC layer thickness of both joints increases as the roll pressure is increased from 100 to 150 MPa. This is because increment of the roll pressure augments the contact between the zinc coated steel and A6000 sheet in this region. In contrast, the IMC layer thickness decreases as the roll pressure is increased from 150 to 175 MPa. This reason is considered as follows.

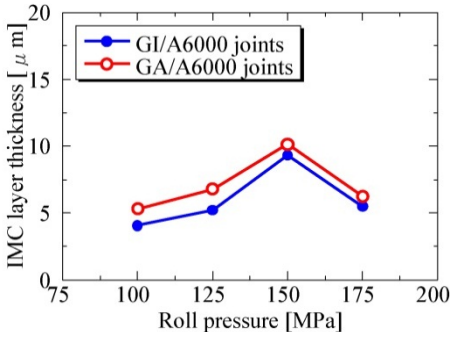

Figure 16. Effect of roll pressure on IMC layer thickness of Laser Roll Welded joints interface

The zinc coated steel and the A6000 sheet contact most widely at roll pressure of 150 MPa. However, when the roll pressure becomes more than 150 MPa, the steel sheet might be curved greatly by high roll pressure. Thus, it's thought that the contact area between the zinc coated steel and the A6000 sheet is narrowed in this region.

3.7. Effect of types of zinc coated steel on thickness of intermetallic compound layer

As shown in Fig.16, the IMC layer thickness of GA/A6000 joints is thicker than that of GI/A6000. This difference is attributed to the evaporation of zinc on the surface of each zinc coated steel sheets.

The boiling point of aluminum, iron and zinc are 2477 °C, 2887 °C and 906 °C respectively, that of zinc is far below those of aluminum and iron. Hence, the zinc on the surface of zinc coated steel sheet is melting, heat of fusion of 7.12 kJ/mol, and evaporating, heat of vaporization of 113.4 kJ/mol (The Japan Institute of Metals, 2004), in the process of Laser Roll Welding. However, because of the zinc on the surface of the GA sheet exists as Fe-Zn alloy, it's hard to be evaporated by the laser heating. Thus, laser energy is little-used for the zinc evaporation, and heat is conducted to A6000 sheet. On the other hand, the zinc on the surface of the GI sheet is easier to be evaporated than that of the GA. Therefore, it's thought that more laser energy for the zinc evaporation is used, and the heat conduction to A6000 sheet decreases.

3.8. Discussion of formation of intermetallic compound layer by thermal cycle at weld interface

Thermal cycle at the weld interface was measured to discuss about the effects of the welding speed and the roll pressure on the IMC layer thickness of Laser Roll Welded joints. The

results of GI/A6000 and GA/A6000 joints at constant roll pressure of 150 MPa is shown in Fig.17 (a) and (b), respectively.

When the welding speed increases from 5.0 to 11.7 mm/s, different thermal cycles were obtained as shown in Fig.17 (a) and (b). Then, in order to quantitative the shape of these thermal cycles, peak temperature and holding time more than 500 °C were focused on.

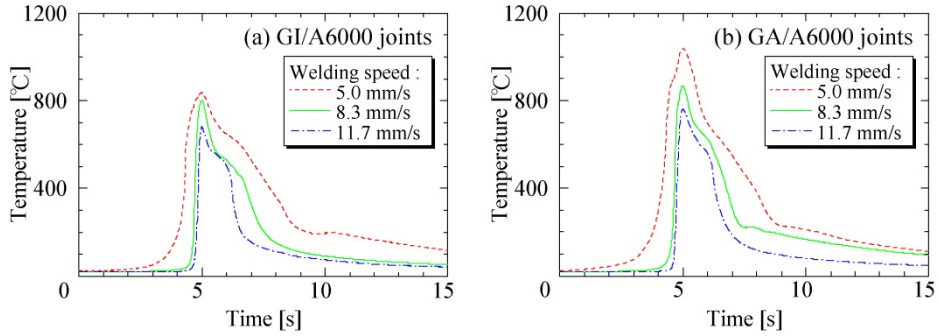

Figure 17. Effect of welding speed on interface thermal cycles of Laser Roll Welded joints

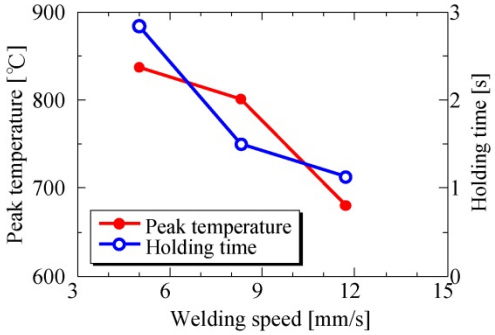

Figure 18. Effect of welding speed on peak temperature and holding time more than 500 °C at interface of GI/A6000 joints

The peak temperature and the holding time more than 500 °C of the thermal cycles in Laser Roll Welding of the GI and the A6000 at different welding speeds are shown in Fig.18. When the welding speed is increased from 5.0 to 11.7 mm/s, the peak temperature decreases from 850 to 680 °C, and the holding time more than 500 °C shortens from 2.8 to 1.1 sec at the weld interface. Hence the reduction of the IMC layer thickness by the increment of welding speed was attributed to the decline of the peak temperature and the shortening of the holding time. The similar results were obtained in Laser Roll Welding of the GA and the A6000.

When the welding speed is slow, there is excessive heat input and the cooling rate is slow. This provides surplus time for the formation of a thick interlayer containing a large amount of the Al-rich brittle IMC's. When the welding speed is fast, there is suitable heat and time

for melting of the aluminum and the diffusion process to take place. Therefore, it's thought that the change of the thermal cycle at the interface affect the formation of the IMC layer when the welding speed is varied.

In addition, when Fig.17 (a) is compared with (b), the peak temperatures of GA/A6000 joints are higher than those of GI/A6000. This fact caused the formation of thicker IMC layer in GA/A6000 joints than in GI/A6000 as shown in Fig.16.

Effect of the roll pressure on the interface thermal cycles of GA/A6000 joints at constant welding speed of 8.3 mm/s is shown in Fig.19. Thermal cycles are shown in Fig.19 (a) and the peak temperature and the holding time more than 500 °C of them are in (b). The reason of the changing of IMC layer thickness by the increment of the roll pressure as shown in Fig.16 is considered by using Fig.19.

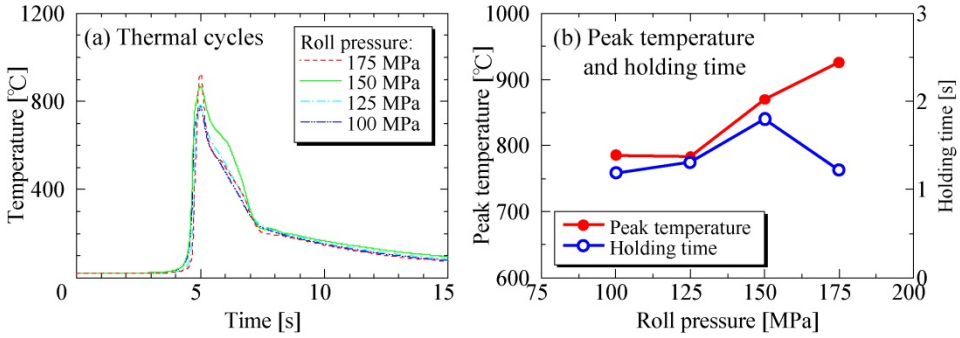

Figure 19. Effect of roll pressure on interface thermal cycles of GA/A6000 joints

From 100 to 150 MPa, the peak temperature and the holding time increase as the roll pressure is increased in Fig.19. Hence the IMC layer thickness increased as the roll pressure is increased in Fig.16. This is because increment of the roll pressure augments the contact between zinc coated steel and A6000 sheet in this region as above. In contrast, from 150 to 175 MPa, the peak temperature rises, but holding time shortens as the roll pressure is increased in Fig.19. It's supposed that this tendency caused the decrement of IMC layer thickness as the roll pressure is increased at high region in Fig.16.

3.9. Results of tensile shear test

Tensile shear test was conducted to investigate the influence of the welding conditions on the weldability. The tensile shear specimens were prepared by cutting the welded specimen with 20 mm width.

Fig.20 shows the tensile shear specimen after testing of GI/A6000 joints. Failure in base metal of the GI sheet is shown in Fig.20 (a), and failure in interface is shown in (b). It's

found that the base-metal-failure specimen failed far from the weld bead as shown in Fig.20 (a).

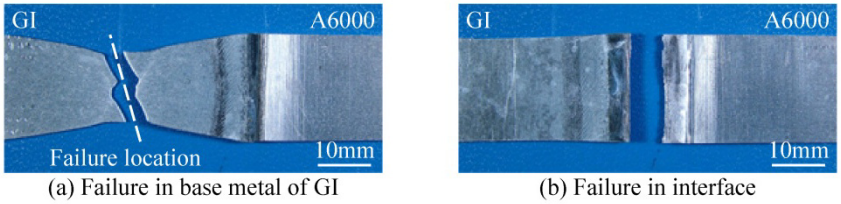

(a) Failure in base metal of GI (b) Failure in interface

Figure 20. Tensile shear specimen after testing of GI/A6000 Laser Roll Welded joints

Results of tensile shear test of GI/A6000 and GA/A6000 joints at various welding speed with the roll pressure of 150 MPa is shown in Fig.21 (a) and (b), respectively. Here the tensile shear strength was converted into the tensile shear load per millimeter of weld length, N/mm, as adopted by Peyre et al. (2007) and Sasabe et al. (2007). Failure in the base metal of the zinc coated steel sheet is shown as a circle in the figure, and failure in interface is shown as a solid mark.

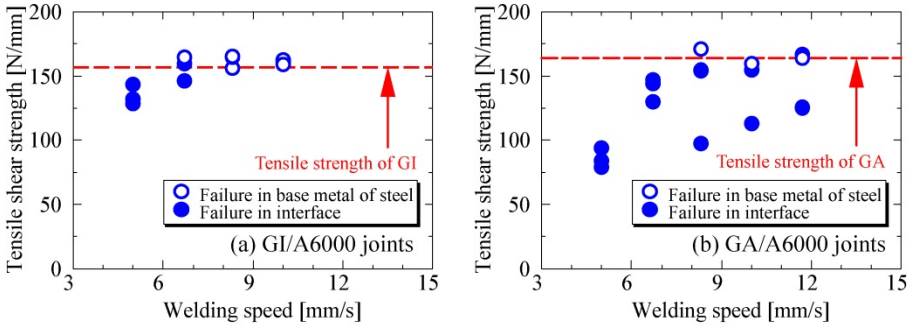

Figure 21. Effect of welding speed on tensile shear strength for Laser Roll Welded joints

When the welding speed is between 6.7 and 10.0 mm/s, the tensile shear strength shows high, and there are many specimens failed in the base metal. This result indicates that the IMC layer thickness is appropriate at these welding speeds. As shown in Fig.21 (a), specimens failed in the base metal could be obtained from 6.7 to 10.0 mm/s. In this region, the IMC layer thickness was less than 10 μm, and failure of specimen occurred in the base metal of the steel sheet. Therefore, it's thought that the IMC layer thickness should be less than 10 μm to get a good joint. As shown in Fig.21 (b), specimens failed in base metal were confirmed when the IMC layer thickness was less than 10 μm. This result corresponded to the articles by other researchers (Bruckner, 2005; Furukawa, 2005).

Additionally, when Fig.21 (a) is compared with (b), the tensile shear strength of GA/A6000 joints is lower than those of GI/A6000. There are three points which can be considered as this reason.

The first is the bonding width of GA/A6000 joints was narrower than that of GI/A6000 as shown in Fig.9. Therefore, when tensile shear load was applied to the joints with narrow bonding width, the load concentrated to the weld. The second is the IMC layer thickness of GA/A6000 joints was thicker than that of GI/A6000 as shown in Fig.16. Moreover, the IMC layers were mainly composed of Al-rich brittle IMC's from the results of the EPMA and the Vickers hardness. The third is the residual zinc at the interface of GA/A6000 joints influenced the tensile shear strength. From the results of the EPMA, a lot of zinc was remained as Fe-Zn alloy layers at the interface of GA sheet side. The zinc coated layer of the GA sheet is formed from the steel side in order of Γ-phase (Fe_3Zn_{10}), Γ_1- (Fe_5Zn_{21}), δ- ($FeZn_7$) and ζ- ($FeZn_{13}$) (The Iron and Steel Institute of Japan, 1982). Since each phase has a difference in generation speed, the Γ-phase is thin and alloy layers are composed mostly of δ- and ζ-. Their phases are hard and brittle. Therefore, the interface of the GA/A6000 joints is weaker than that of the GI/A6000.

The maximum tensile shear strength of GI/A6000 joint, 162 N/mm, was obtained at the welding speed of 8.3 mm/s and the roll pressure of 150 MPa. This strength is equal to the tensile strength of the GI sheet, 157 N/mm, and 63% of the A6000 sheet, 256 N/mm. On the other hand, the maximum strength of GA/A6000 joint, 160 N/mm, was obtained at the welding speed of 10.0 mm/s and the roll pressure of 100 MPa. This strength is equal to the tensile strength of the GA sheet, 164 N/mm, and 62% of the A6000 sheet, 256 N/mm.

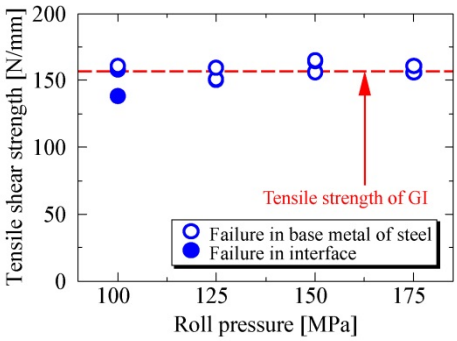

Figure 22. Effect of roll pressure on tensile shear strength for GI/A6000 joints

In addition, results of tensile shear test at various roll pressure with welding speed of 8.3 mm/s is shown in Fig.22. All specimens were failure in the base metal of the GI sheet except for the roll pressure 100 MPa. It's considered that the IMC layer thickness is less than 10 μm at these roll pressures as shown in Fig.16. Therefore, it seems that there is little influence of the roll pressure on the tensile shear strength.

3.10. Discussion of relation between intermetallic compound layer thickness and tensile shear strength

From the above results, it has became clear that there is a close relation to the IMC layer thickness to the tensile shear strength also in Laser Roll Welding of zinc coated steel and aluminum alloy. There, the relationship between the IMC thickness and the tensile strength was discussed about all joints in this experiment. Effect of the IMC layer thickness on the tensile shear strength of GI/A6000 and GA/A6000 joints with different welding speed and roll pressure is shown in Fig.23 (a) and (b), respectively.

As above, only when the IMC layer thickness was less than 10 μm, the base-metal-failure specimens were obtained. When the IMC layer thickness is from 4 to 6 μm, high tensile shear strength could be obtained. When the IMC layer is thicker than 6 μm, the tensile strength is decline. This is because the increment of the brittle IMC's at the joint interface might lead to weaken of the welded joint, and the joint isn't able to resist a heavy load.

On the other hand, when the IMC layer is thinner than 4 μm, the tensile strength also declines. In this case, due to low heat input might lead to incomplete welding at the joint interface. As shown in Fig.9, the bonding width is decreased by the decrement of the heat input.

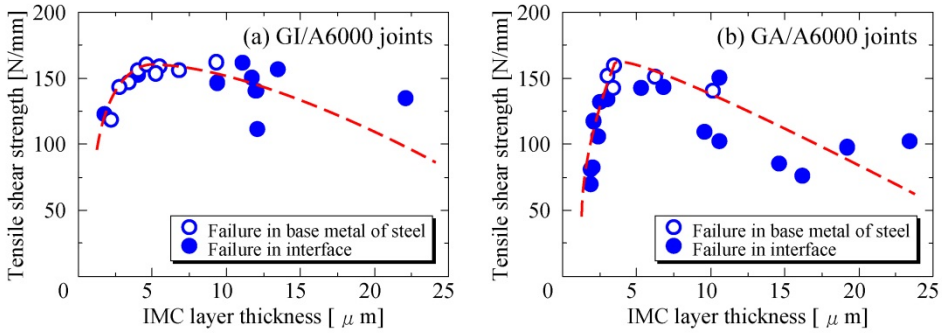

Figure 23. Effect of IMC layer thickness on tensile shear strength for Laser Roll Welded joints

3.11. Results of Erichsen cupping test

Finally, in order to investigate the formability of GI/A6000 and GA/A6000 joints, Erichsen cupping tests were carried out. The specimens were prepared by cutting the welded joints with the welding speed of 8.3 mm/s and roll pressure of 150 MPa into 77 mm square. A punch is pushed into the specimen. When the specimen is failed somewhere, the cupping height is evaluated as Erichsen value.

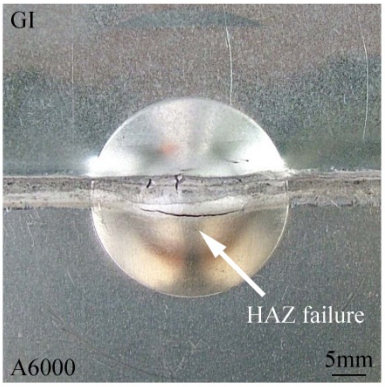

Figure 24. Erichsen cupping test specimen after testing of GI/A6000 joint

The Erichsen cupping test specimen after testing of GI/A6000 joint is shown in Fig.24. The specimen was failed at HAZ of the A6000 sheet side and the Erichsen value was 7.9 mm. With the GI base metal, the Erichsen value was 11.9 mm; with the A6000 base metal, the value was 8.6 mm. Therefore, this value was 92% of the base metal of A6000 sheet. In contrast, the specimen of GA/A6000 joint was failed at interface and the value was 3.6 mm. The same tendency was seen in the tensile shear test.

4. Conclusions

The present study is focused on the dissimilar metal joining of zinc coated steel and aluminum alloy by Laser Roll Welding. The following conclusions can be drawn.

1. The IMC layer was observed at the interface of all welded joins. It was suggested that most of the IMC's are brittle $FeAl_3$ and Fe_2Al_5 from the results of EPMA and Vickers hardness measurement. As the welding speed was faster than 10.0 mm/s, zinc was confirmed in aluminum alloy.
2. Increase in the welding speed led to decrease the bonding width and the IMC layer thickness at the joint interface. When the roll pressure was increased, the IMC thickness at the pressure of 150 MPa was the thickest. The IMC layer thickness of GA/A6000 joints was thicker than that of GI/A6000 on the whole.
3. Increase in the welding speed led to lowering of the peak temperature and shortening of the holding time more than 500 ^{o}C at the interface. The peak temperature at the roll pressure of 175 MPa was the highest, and the holding time at the pressure 150 MPa was the longest. The peak temperature of GA/A6000 joints was higher than that of GI/A6000 at the same welding condition.
4. When the IMC layer was less than 10 μm, failure of specimen occurred at the base metal of zinc coated steel in tensile shear test. The joint properties of GI/A6000 joints were better than those of GA/A6000 from the results of tensile shear test and Erichsen cupping test.

5. The welding speed influenced the joint performance such as the IMC layer thickness and the tensile shear strength to a greater degree than the roll pressure in Laser Roll Welding.

Author details

Hitoshi Ozaki
Graduate School of Engineering, Mie University, Japan

Muneharu Kutsuna
Advanced Laser Technology Research Center Co., Ltd., Japan

Acknowledgement

The authors would like to thank Mr. S. Nakagawa and Mr. K. Miyamoto from Research Center, Nissan Motor Co., Ltd. for their support in this research.

5. References

Bruckner, J. (2005). Cold Metal Transfer Has a Future Joining Steel to Aluminum. *Welding Journal*, Vol.84, No.6, pp.38-40, ISSN 0043-2296

Dharmendra, C., Rao, K. P., Wilden, J. & Reich, S. (2011). Study on Laser Welding-brazing of zinc Coated Steel to Aluminum Alloy with a Zinc Based Filler. *Material Science and Engineering A*, Vol.528, pp.1497-1503, ISSN 0921-5093

Fan, J., Thomy, C. & Vollertsen, F. (2011). Effect of Thermal Cycle of the Formation of Intermetallic Compounds in Laser Welding of Aluminum-Steel Overlap Joints. *Physics Procedia*, Vol.12, pp.134-141, ISSN 1875-3892

Furukawa, K. (2005). Welding Process of Iron-Aluminum. *Welding Technology*, Vol.53, No.8, pp.94-102, ISSN 0387-0197

Katayama, S. (2004). Laser Welding of Aluminum Alloys and Dissimilar Metals. *Journal of Light Metal Welding & Construction*, Vol.42, No.1, pp.16-25, ISSN 0368-5306

Katoh, K. & Tokisue, H. (2004). Dissimilar Friction Welding of Aluminum Alloys to Other Materials. *Journal of Light Metal Welding & Construction*, Vol.42, No.2, pp.11-18, ISSN 0368-5306

Massalski, T. B. (1986). *Binary Alloy Phase Diagrams Volume 1*, American Society for Metals, p.148, ISBN 0871702614, Ohio

Nishimoto, K., Atagi, K., Fujii, H. & Katayama., S. (2005). Laser Pressure Welding of Dissimilar Metals Welding. *Proceedings of the 63rd Laser Materials Processing Conference*, pp.133-138, ISBN 4947684585, May, 2005

Ohashi, O. (2004). Diffusion Bonding of Aluminum to Different Metals. *Journal of Light Metal Welding & Construction*, Vol.42, No.2, pp.19-23, ISSN 0368-5306

Okamura, H. & Aota, K. (2004). Joining of Dissimilar Materials with Friction Stir Welding, *Journal of Light Metal Welding & Construction*, Vol.42, No.2, pp.1-10, ISSN 0368-5306

Okita, T. (2004). Resistance Welding of Aluminum Alloys to Dissimilar Metals. *Journal of Light Metal Welding & Construction*, Vol.42, No.1, pp.2-15, ISSN 0368-5306

Ozaki, H., Hayashi S. & Kutsuna M. (2008). Laser Roll Welding of Dissimilar Metal Joint of Titanium to Aluminum Alloy. *Quarterly Journal of Japan Welding Society*, Vol.26, No.1, pp.24-30, ISSN 0288-4771

Ozaki, H., Ichioka R. & Kutsuna M. (2007). Laser Roll Welding of Dissimilar Metal Joint of Low Carbon Steel and Titanium. *Quarterly Journal of Japan Welding Society*, Vol.25, No.1, pp.173-178, ISSN 0288-4771

Ozaki, H. & Kutsuna M. (2007). Laser Roll Welding of Dissimilar Metal Joint of Low Carbon Steel to Aluminum Alloy Using 2kW Fiber Laser. *Quarterly Journal of Japan Welding Society*, Vol.25, No.4, pp.473-479, ISSN 0288-4771

Peyre, P., Sierra, G., Deschaux-Beaume, F., Stuart, D. & Fras, G. (2007). Generation of Aluminum-steel Joints with Laser-induced Reactive Wetting. *Material Science and Engineering A*, Vol.444, pp.327-338, ISSN 0921-5093

Rathod, M. & Kutsuna M. (2003). Laser Roll Bonding of A5052 Aluminum Alloy and SPCC Steel. *Quarterly Journal of the Japan Welding Society*, Vol.21, No.2, pp.282-294, ISSN 0288-4771

Rathod, M. J. & Kutsuna M. (2004). Joining of Aluminum Alloy 5052 and Low-Carbon Steel by Laser Roll Welding. *Welding Journal*, Vol.83, No.1, pp.16s-26s, ISSN 0043-2296

Sasabe, S., Iwase, T., Matsumoto, T., Hattori, Y. & Miono, T. (2007). Dissimilar Metal Joining of Aluminum Alloys to Steel by using Newly-developed Hot-dip Aluminized Steel Sheet. *Journal of Light Metal Welding & Construction*, Vol.45, No.2, pp.23-33, ISSN 0368-5306

Satou, D. (2004). Aluminum Clad of Explosive Welding. *Journal of Light Metal Welding & Construction*. Vol.42, No.1, pp.26-30, ISSN 0368-5306

The Iron and Steel Institute of Japan (1982). *Iron and Steel Handbook Vol. 6 (3rd Edition)*, Maruzen, pp.421-434, Tokyo

The Japan Institute of Metals (2004). *Metals Data Book (Revised 4th Edition)*, Maruzen, p.11, ISBN 4621073672, Tokyo

Torkamany, M., Tahamtan, S. & Sabbaghzadeh, J. (2010). Dissimilar Welding of Carbon Steel to 5754 Aluminum Alloy by Nd:YAG Pulsed Laser. *Materials and Design*, Vol.31, pp.458-465, ISSN 0261-3069

Yamamoto, S. (2012). Welding in the World –Picking up from Foreign Magazine. *Welding Technology*, Vol.60, No.3, (2012), p. 75, ISSN 0387-0197

Yan, S., Hong, Z., Watanabe, T. & Jingguo, T. (2010). CW/PW Dual-beam YAG Laser Welding of Steel/Aluminum Alloy Sheets. *Optics and Lasers in Engineering*, Vol.48, pp.732-736, ISSN 0143-8166

Yasuyama, M., Ogawa, K. & Taka, T. (1996). Spot welding of aluminum and steel sheet with insert of aluminum clad steel sheet – Part 1. *Quarterly Journal of Japan Welding Society*, Vol.14, No.2, pp.314-320, ISSN 0288-4771